Fuel Cell Performance of Non-Precious Metal Based Electrocatalysts

Yan-feng ZHANG

Fei XIAO

Guang-yu CHEN

Min-hua SHAO
2. Department of Chemical and Biological Engineering, Hong Kong University of Science and Technology, Clear Water Bay, Kowloon, Hong Kong, China;5. Fok Ying Tung Research Institute, The Hong Kong University of Science and Technology, Guangzhou 511458, China;6. Energy Institute, The Hong Kong University of Science and Technology, Clear Water Bay, Kowloon, Hong Kong 999077, China;, kemshao@ust.hk

基于非贵金属氧还原催化剂的
质子交换膜燃料电池性能

张焰峰 [1,2,3,4a],肖　菲 [2a],陈广宇 [2,5a],邵敏华 [2,5,6*]

(1. 江苏奥新新能源汽车有限公司,江苏 盐城 224000;2. 香港科技大学化学及生物工程系,香港 九龙清水湾;
3. 上海智能新能源汽车科创功能平台有限公司,上海 201805;4. 长三角新能源汽车研究院有限公司,江苏 盐城;
5. 广州市香港科大霍英东研究院,广东 广州 511458;6. 香港科技大学能源研究院,香港 999077)

摘要: 质子交换膜燃料电池的成本和寿命问题是制约其商业化的主要瓶颈. 开发高效稳定的新型非铂氧还原催化剂是降低电池成本的重要途径. 过渡金属-氮-碳型非贵金属催化剂具有较高催化活性、资源丰富、价格低廉等优点, 被认为是未来最有希望替代铂的氧还原催化剂. 本综述从催化剂的设计构筑、催化层结构优化以及电池测试等方面, 对过渡金属-氮-碳型非贵金属催化剂的国内外最新研究进展进行了重点讨论, 并对未来其发展趋势提出展望.

关键词: 质子交换膜燃料电池;非贵金属催化剂;膜电极;耐久性

中图分类号: O646.7;TM911.4　　　　　　　　　　　　　　**文献标识码:** A

氢气作为新的能源载体将彻底改变当今社会以煤、石油、天然气等不可再生资源为主的传统能源结构. 氢气的制备、存储、运输与再利用等相关技术开发是构建零碳氢能社会的基础. 质子交换膜燃料电池 (proton exchange membrane fuel cells, PEMFCs)是氢能源转化利用的最佳方式,其不经过燃烧, 直接以电化学反应的方式将氢燃料中的化学能转化为电能,具有清洁高效、工作温度低、启动速度快等突出优点, 在新能源汽车和分布式发电领域具有非常广阔的应用前景[1]. PEMFCs 相关技术和产业链的开发受到了各国政府、能源企业和汽车厂商的广泛青睐.

经过全球近六十年的研发, PEMFCs 取得了很多技术上的突破. 目前制约其大规模商业化应用的主要瓶颈是高昂成本和较短寿命. PEMFCs 成本高的一个主要原因是贵金属 Pt 在催化剂层的大量使用. 与快速的阳极氢气氧化反应(hydrogen oxidation reaction,HOR)相比,PEMFCs 的阴极氧气还原反应(oxygen reduction reaction,ORR)非常迟缓, 为保证电池输出性能和较高的能量转换效率, 需要

使用大量 Pt 作为催化剂[2-4]. 美国能源部(US DOE)预测, 即使以现有最好的技术大规模量产 PEMFCs,Pt 基催化剂的成本也要占整个 PEMFCs 电堆成本的 40% 以上. 此外,Pt 基纳米催化剂在强酸性、高电位、强氧化的反应条件下稳定性较差. PEMFCs 运行过程中 Pt 基纳米粒子会发生溶解、团聚, 碳载体腐蚀会导致 Pt 纳米粒子脱落, 使 Pt 基催化剂的 ORR 活性不断降低,严重影响电堆的使用寿命[5-7].

开发廉价、高效稳定的新型非 Pt 氧还原催化剂, 摆脱对稀缺 Pt 资源的依赖, 从而降低电池成本、延长其运行寿命是实现 PEMFCs 商业化的重要途径. 在诸多非贵金属催化剂中,资源丰富、价格低廉的过渡金属-氮-碳(M-N-C,M 主要是 Fe 和 Co)型催化剂由于其具有相对较高的 ORR 活性和稳定性,被认为是未来最有希望替代 Pt 的 ORR 催化剂[8-11]. 尤其是 Fe-N-C 催化剂, 实际燃料电池测试其 ORR 动力学电流密度已不断接近商业 Pt/C 催化剂. 然而,M-N-C 型催化剂具有 ORR 活性的 $M-N_x$ 位点密度低,单位体积比活性较低,为了减小

电化学极化、获得与 Pt 催化剂相当的 ORR 活性,制备膜电极(membrane electrode assembly, MEA)时不得不加大其使用量. 催化剂载量增加势必会增大膜电极阴极催化层 (cathode catalyst layer, CCL)的厚度,使电极内部的质量和电荷传输阻力增大,严重影响电池的性能输出[12-16]. 针对这一亟待解决的关键问题,本文将从催化剂自身的设计构筑、阴极催化层的结构组成优化,电池运行条件以及耐久性四个方面,对 M-N-C 型非贵金属 ORR 催化剂的国内外最新研究进展进行详细评述.

1 M-N-C 型催化剂设计构筑

表 1 列举了 2016-2020 年 M-N-C 型催化剂膜电极制备工艺、测试参数以及燃料电池性能. 由于非贵金属催化剂的活性位点少,在制备膜电极时需要比较高的催化剂载量 (3 ~ 4 mg·cm^{-2}). 通常 1 mg·cm^{-2} 载量的催化剂层的厚度为 20 ~ 25 μm,因此非贵金属催化剂的阴极催化层的厚度为 80 ~ 100 μm, 远远大于铂基阴极催化剂的厚度 (< 10 μm)[4]. 厚重的阴极催化层严重的影响了燃料电池测试中氧气的传输效率, 因此为了减少传输阻力,在非贵金属催化剂合成过程对孔隙的调控并增加表面积对提高燃料电池性能尤其是在高电流放电区域具有重要意义[17-18]. 其中在合成过程中引入二氧化硅[19]、氧化镁[20]等硬模板[21]是最普遍直接的方法. 金属模板法(如 ZIF-8)是通过金属和配体的螯合作用形成一定孔隙结构的前驱体,并利用锌在热处理过程中(> 907 ℃)的升华原位形成孔隙来制备多孔的催化剂. Barkholtz 等[22]比较了来源于不同铁源(醋酸亚铁(Fe(Ac)$_2$),高氯酸亚铁(TPI),有机配体(1,10-菲咯啉)与金属框架(Zn(ImI)$_2$)前驱体制备的 Fe-N-C 催化剂. 其中直接在 Zn(ImI)$_2$ 加入高氯酸亚铁(TPI)合成的 Zn(mIm)$_2$TPI 拥有最高的表面积(859.3 m^2·g^{-1})和功率密度(0.603 W·cm^{-2})(图 1A-B). Zhao 等[23]固定高氯酸亚铁(TPI)作为统一铁源,比较由不同的有机配体(2-甲基咪唑(mIm),咪唑(Im),2-乙基咪唑(eIm),4-氮杂苯并咪唑(4abIm))形成的金属有机框架对 Fe-N-C 催化剂性能的影响,Zn(mIm)$_2$IPI 前驱体的表面积(2065 m^2·g^{-1})远超其他配体, 其热解后的催化剂在燃料电池中具有最高的功率密度(图 1C). 由此可以看出,非贵金属催化剂的表面积依赖于金属与配体之间的相互作用且影响其燃料电池性能. 除了设计交错的孔隙结构和增加表面积, 尽可能地让非贵金属的活性位点暴露在界面也是至关重要的. 因为无论是传统的物理混合法还是金属有机模板法,在热处理中金属位点容易形成碳包裹无法接触反应物质. 对碳载体缺陷的设计调控以提高活性位点的利用率, 有助于提高非贵金属催化剂的燃料电池的体活性并提高电压下的电流密度.

从表 1 中可以发现,Fe-N-C 和 Co-N-C 是被研究最为广泛的非贵金属催化剂. 在纯氧条件下的燃料电池测试中,由二氧化硅与金属模板共同制备的 Fe-N-C(TPI@Z8(SiO$_2$)-650-C)催化剂和通过表面活性剂的保护下制备的 Co-N-C(Co-N-C@F127) 催化剂可以分别达到 1.18[10]和 0.87 W·cm^{-2}[48]的功率密度(图 2A-B),是已知报道中最高纪录. 非贵金属催化剂的最高功率密度一般在 0.3 ~ 0.4 V 的电压下实现,而 Barkholtz 等[22]和 Li 等[29]报道的 Fe-N-C 催化剂在 0.55 V 的电压下分别实现了 0.60 和 1.01 W·cm^{-2}的功率密度. 由于质子膜燃料电池的通常的应用电压为 0.6 ~ 0.7 V,表 1 归纳了不同非贵金属催化剂在 0.6 V 电压下的功率密度情况. 对比发现,0.6 V 电压下的功率密度通常比最高功率密度低 0.1 ~ 0.2 W·cm^{-2},非贵金属催化剂的最高功率相同或相近并不意味着 0.6 V 时的功率密度也相同或相近. 该电压下的功率密度,不仅取决于催化剂本身表面积和活性位点的分布, 同时取决于催化层氧气传输和质子传输的协同作用. 从实际应用角度分析,提高阴极催化剂在 H$_2$-Air 中的性能更能推动燃料电池的商业化. 但是因为厚重的非贵金属催化剂层,空气测试中物质传输问题会比氧气测试中严重. 基于少数空气燃料测试结果分析发现,将测试气体从氧气转换成空气,最高功率密度将降低超过两倍. 目前,Fe-N-C 催化剂在 H$_2$-Air 测试环境的中一般可实现 0.3 ~ 0.4 W·cm^{-2} 最大功率密度.

DOE 对非贵金属催化剂设定的活性目标为在 2020 年实现在 0.9 V 产生大于 0.044 A·cm^{-2} 的电流密度(H$_2$/O$_2$). 目前,通过两种不同氮源(聚苯胺和氰胺) 合成的具有层级多孔结构的 Fe-N-C 催化剂在 0.87 V 的电压下实现了 0.044 A·cm^{-2} 的电流密度[35]. 而通过二氧化硅和金属有机框架的协同作用制备多孔 Fe-N-C 催化剂在 0.88 V 的电压下实现 0.047 A·cm^{-2} 的电流密度[10]. 因此,优化孔隙结构和增加活性位点的密度和利用率,对实现活性目标至关重要.

表 1　非贵金属催化剂质子膜燃料电池催化剂膜电极制备参数,测试条件及测试结果.

Tab. 1　Comparisons in membrane electrode assembly synthesis, proton exchange membrane fuel cell measurement condition and relative performance of non-precious metal based electrocatalysts.

Type	Ref.	Catalyst loading/ (mg·cm⁻²)	I/C weight ratio	Panode & Pcathode/ bar	H₂/O₂/Air/ (mL·min⁻¹)	H₂-O₂ power density/(W·cm⁻²)		Power density (at 0.6 V)	H₂-air power density/ (W·cm⁻²)	
						Maximum			Maximum	
						Power density	Voltage/ V		Power density	Voltage/V
	[24]	3.5	0.85	1.0	200/200				0.32	0.6
	[25]	2.2		1.5	400/400	0.62	0.46	0.42		
	[22]	4.0	0.7	1.0		0.60	0.55	0.56		
	[26]	3.5		1.0	200/200	0.67		0.52		
	[27]	4.1	1	1.5	300/300	0.73	0.4	0.55		
	[23]	2.2	1	1.5	300/400	0.62	0.43	0.41		
	[28]	3.0	1.5	2.0	300/400	0.9	0.45	0.72		
	[29]	2.0	1	1.5	200/240	1.01	0.55	0.80		
	[30]	3.5	0.6	1.5	200/200	1.1	0.4	0.71		
	[31]	4.0		1.0	60/60/200	0.43	0.45	0.18	0.32	0.48
	[20]	3.0	1	1.0	250/300	0.63	0.41	0.5		
	[32]	4.0	0.46		200/350	0.66	0.44	0.4		
	[33]	3.0	0.45	2.0	250/200/200	0.49	0.4	0.4	0.32	0.5
Fe-N-C	[19]	3.0		1.0	300/300				0.32	0.48
	[10]	2.0	1.3	1.0	300/400/500	1.18	0.47	1.03	0.43	0.53
	[34]	0.77		1.5	1.5/2.5	0.85	0.4	0.6		
	[35]	4	0.55	1.5	200/200/200	0.94	0.4	0.68	0.42	0.5
	[36]	3	0.66	1.0	150/150	0.45	0.3	0.23		
	[37]	3	0.3	1.0	400/1200	0.55	0.4	0.36		
	[38]	4	0.55	2.0	400/400	0.7	0.35	0.33		
	[39]	3.5	0.54	2.0	200/200/200	0.7	0.41	0.52	0.32	0.52
	[40]	4	0.83	1.0	200/200/300	0.68	0.38	0.47	0.40	0.52
	[41]	4	0.2	1.4	300/400/400	0.86	0.39	0.62	0.43	0.42
	[42]	4	2	0	300/300	0.35	0.42	0.27		
	[43]	4	0.46	1.0	200/200/200	0.63	0.4	0.48	0.36	0.5
	[44]	4	1.25	2.0	300/300/300	0.8	0.48	0.7	0.38	0.5
	[45]	4	1.5	1.5	300/300/300	0.75	0.4	0.63	0.30	0.51
	[46]	1.6	0.86	1.5	200/200	0.37	0.41	0.2		
Co-N-C	[47]	3.0	1	2.0	300/400/400	0.79	0.45	0.65	0.30	0.52
	[11]	4.0	0.54	2.0	200/200/200	0.56	0.38	0.29	0.28	0.45
	[48]	4.0	0.6	1.0	200/200	0.87	0.45	0.60		
Mn-N-C	[49]	4.0	0.35	1.5	200/200/200	0.46	0.3	0.25	0.15	0.48

2　阴极催化层结构组成优化

不仅非贵金属催化剂本身的微观结构会影响燃料电池的性能,膜电极的制备工艺也至关重要.催化剂层的制备通常是将催化剂分散在醇和水的混合溶剂里,并加入一定比例的离聚物,其中离聚物的作用是传导质子协助氧还原反应的进行.离聚物(I)与催化剂(C)的比例(I/C)必须在一个优化的范围,如果 I/C 比例太高,离聚物可能直接覆盖活性位点,造成中毒,使其失去活性.I/C 比例太低会造成电极的质子传输阻力过大.因此,优化非贵金
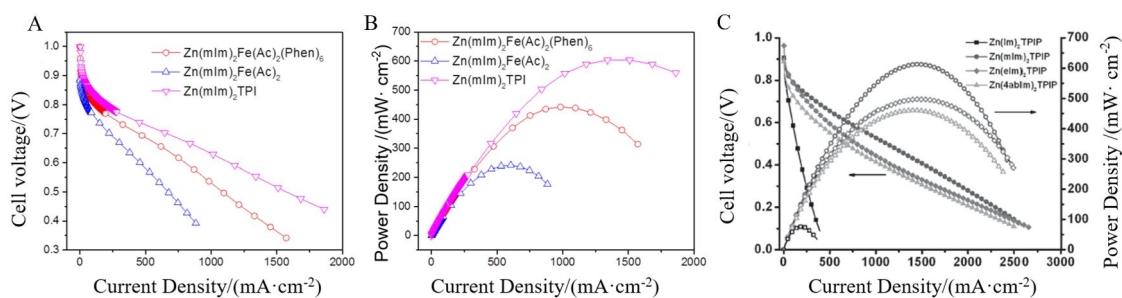
图 1 Zn(mIm)₂Fe(Ac)₂(Phen)₆, Zn(mIm)₂Fe(Ac)₂ 和 Zn(mIm)₂TPI 的(A)电压-电流密度极化曲线和(B)功率-电流极化曲线[22]. (C) Zn(Im)₂, Zn(mIm)₂TPIP, Zn(elm)₂TPIP 和 Zn(4abIm)₂TPIP 的电压-电流密度极化曲线[23].

Fig. 1 (A) Voltage-current density polarization curves and (B) power density-current density curves for Zn(mIm)₂ Fe(Ac)₂(Phen)₆, Zn(mIm)₂Fe(Ac)₂ and Zn(mIm)₂TPI[22]. (C) Voltage-current density and power density-current density curves for Zn(Im)₂, Zn(mIm)₂TPIP, Zn(elm)₂TPIP and Zn(4abIm)₂TPIP[23].
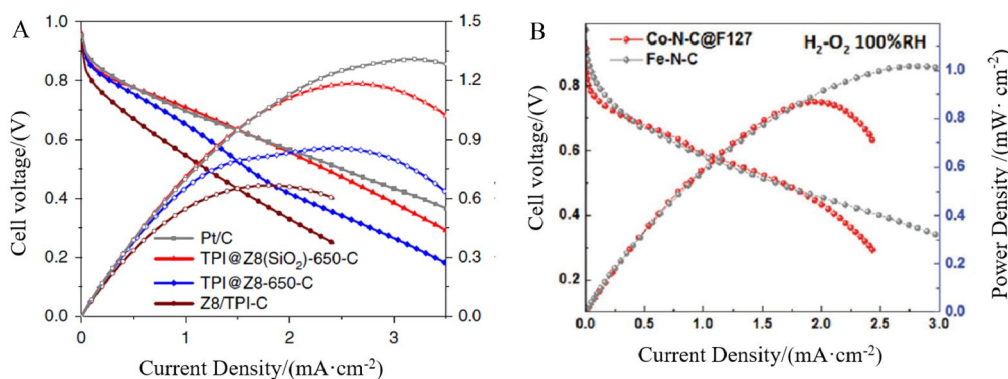

图 2 (A) 目前报道最高功率密度的 Fe-N-C (TPI@Z8(SiO₂)-650-C)极化曲线[10]. (B) 目前报道最高功率密度的 Co-N-C (Co-N-C@F127)极化曲线[48].

Fig. 2 (A) The polarization curves for Fe-N-C (TPI@Z8(SiO₂)-650-C) with the highest reported power density[10]. (B) The polarization curves for Co-N-C (Co-N-C@F127) with the highest reported power density[48].

属催化剂燃料电池性能首先需要完善催化剂浆液的 I/C 比例. 根据表格 1 中的归纳发现 I/C 质量比例跨度范围比较宽 (0.3~2),并没有统一的章法可循, 最优比例可能依赖于非贵金属材料本身的微观结构. Barkholtz 等[24]发现由 ZIF-8 和高氯酸亚铁制备的 Fe-N-C 催化剂在 I/C 比例为 0.85 时达到最大的功率密度. 当比例低至 0.5 或 0.6 时, 燃料电池的整体性能显著降低; 比例高至 1 时, I-V 曲线在高电压的动力学区域影响不大, 但在高电流区域呈现出快速的衰减(图 3A). Shui 等[28]发现通过静电纺丝方法制备的纳米纤维状 Fe-N-C 催化剂在 I/C 比例为 1.5 时,燃料电池性能最优,I/C 比例降低到 1 时仍然保持较好的动力学性能, 但当电压小于 0.6 V 时, 燃料电池性能快速下降. 如图 3B-C 所示,Banham 等[50]固定 40wt.% 离聚物

比例比较不同载量的 Fe-N-C 催化剂层的在 H₂-O₂ 和 H₂-Air 中燃料电池性能. 在空气测试环境下,1 mg·cm⁻² 载量的膜电极在低电流区性能均较差, 但在高电流区域呈现出较好的传质性能,4 mg·cm⁻² 载量的电池性能最差. 在氧气测试环境下,不同载量的性能差异减小,2.5 mg·cm⁻² 载量的膜电极在空气或氧气的测试环境中的性能都最优.

除了催化剂分浆液,催化层的制备工艺同样也影响膜电极的性能. 目前催化层的制备主要有三种方法,分别是直接刷或喷到气体扩散层(常用的是 Sigracet 25 BC)[10, 22, 24, 36, 38, 42, 44, 47-48]或质子膜上[30, 39-41, 49]或先喷涂到 PTFE 膜上再转印到质子膜上[11, 34, 37]. 催化剂浓浆直接刷涂到气体扩散层的方法较为普遍, 但是在热压到质子膜时需要先对催化层表面进行修平, 防止热压过程中催化层的凸
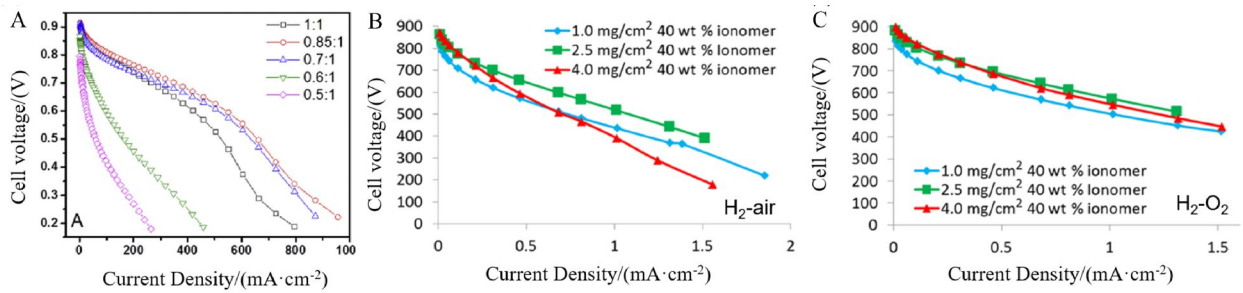
图 3　(A) Fe-N-C 催化剂不同 I/C 比例的电压-电流密度极化曲线[24]. Fe-N-C 催化剂在 40wt.%离聚物比例下，不同载量的膜电极在(B)H₂-air 和(C)H₂-O₂ 燃料电池测试下的电压-电流密度极化曲线[50].

Fig. 3　(A) The voltage-current density polarization curves for Fe-N-C with different I/C ratios[24]. Voltage-current density polarization curves recorded in (B) H₂-air and (C) H₂-O₂ environments for Fe-N-C with 40wt.% ionmer ratio and different catalyst loadings[50].

起破坏质子交换膜. 由于气体扩散层存在一定的孔隙结构，催化剂浓浆有可能堵塞扩散层孔隙，影响气体的传输. 将催化剂浆料刷（喷）到质子膜上可以简化热压步骤，同时加强催化层与膜之间的相互接触减少传输阻力，但需要特殊的夹具设计避免质子膜的在接触浓浆时发生膨胀和变形. 将催化剂间接喷涂在 PTFE 基底上可以使得催化剂分散相对均匀，但将催化层转印到质子膜的过程中会造成一部分未成功转印的催化剂损失，且相比前两种方法多一步热压过程，容易造成催化剂层孔洞结构的崩塌. 综上所述，目前还未有定论何种催化层制备方法最适合非贵金属催化剂，仍需要系统研究.

3　电池运行条件影响
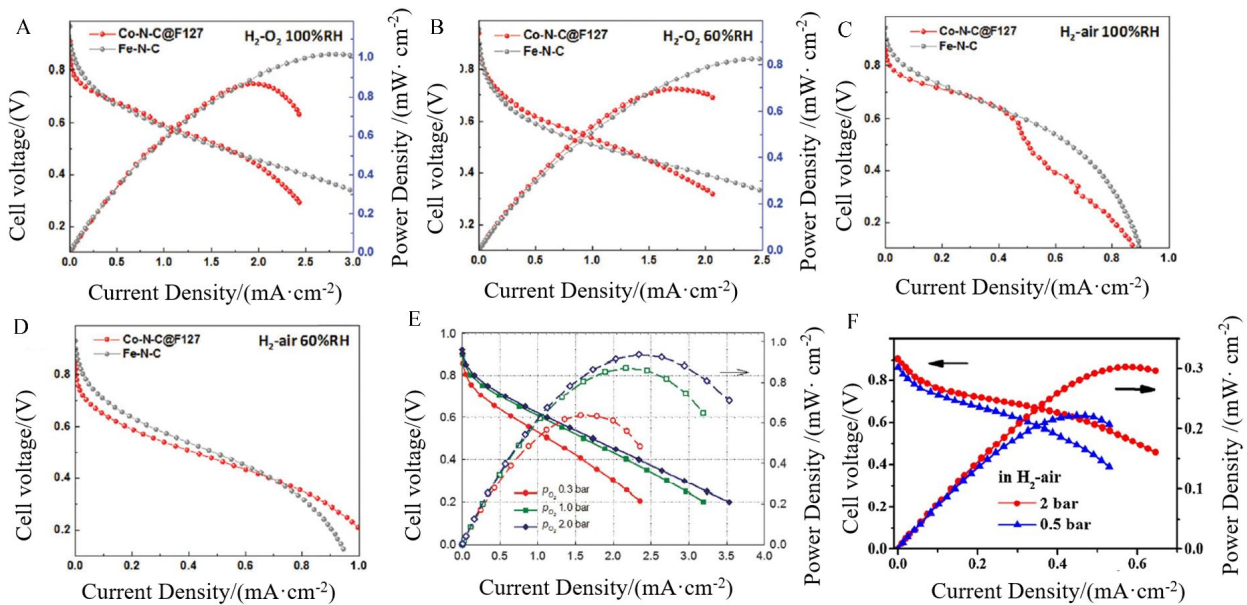
DOE 设定的非贵金属催化剂的燃料电池测试条件为 80 °C、100% 相对湿度和 1.5 bar 压力的纯

图 4　Fe-N-C 和 Co-N-C@F127 催化剂在(A-B) H₂-O₂ 和(C-D) H₂-air 环境(A, C) 100%和(B, D)60%相对湿度的极化曲线对比[48]. (E) Fe-N-C 催化剂在 H₂-O₂ 环境不同测试压力下的极化曲线[35]. (F) Co-N-C 催化剂在 H₂-air 环境不同测试压力下的极化曲线[47].

Fig. 4　The polarization curves for Fe-N-C and Co-N-C@F127 measured at (A-B) H₂-O₂ and (C-D) H₂-air environments, (A, C) 100% and (B, D) 60% relative humidity[48]. (E) The polarization curves for Fe-N-C at H₂-O₂ environment under different pressures[35]. (F) The polarization curves for Co-N-C at H₂-air environment under different pressures[47].

氧环境. 如图 4A-D 所示, He 等[48]发现在氧气环境下将相对湿度从 100% 降低到 60%, 基于非贵金属催化剂(Co-N-C@F127 和 Fe-N-C)的燃料电池性能降低. 在空气环境下, 孔隙率高的 Co-N-C@F127 催化剂在 100% 相对湿度时高电流区域由于水管理失衡造成性能衰减, 将湿度降低到 60% 有利于提升整体燃料电池性能. Chung 等[35]在氧气测试环境下对比分析(CM+PANI)-Fe-C 膜电极在 0.3、1.0 和 2.0 bar 压力下的燃料电池性能. 测试压力从 0.3 bar 增加到 1 bar, 燃料电池的性能呈现明显的提升, 最高功率密度从 0.62 W·cm⁻² 提高到 0.87 W·cm⁻²; 持续增加到 2.0 bar, 功率密度进一步提升达到 0.94 W·cm⁻²(图 4E). Chen 等[47]报道 Co-N-C 催化剂在空气的燃料电池测试中压力从 0.5 bar 提升至 2 bar 上, 最高功率密度从 0.221 W·cm⁻² 提升到 0.305 W·cm⁻²(图 4F). 文献中记录的非贵金属催化剂燃料电池测试压力一般不大于 2 bar, 在此范围内催化剂燃料电池的性能随着压力的增加而提升, 压力过大会造成催化剂层结构的破坏并加速膜电极的退化. 目前, 鲜有对测试过程中气流量影响的探究. 从表 1 中发现, 大部分基于非贵金属催化剂的 PEMFC 性能测试是采取固定气流量的方式, 但气流量的选择并没有统一标准, 其中空气的气流量一般等于或大于氧气的气流量.

4 非贵金属催化剂耐久性分析

目前非贵金属催化剂的耐久性测试主要是在控电压或控电流条件下观测电流密度或电压的变化[51-52]. 近几年来, 尽管非贵金属催化剂的性能得到了提升, 但现有文献报道的膜电极的最高耐久性记录(700 小时)[53]仍与 DOE 设定的 5000 小时目标相差甚远. Chen 等[30]报道的 Fe-N-C 催化剂可以达到 1.1 W·cm⁻², 但在 0.4 V 电压下保持 20 小时就会造成 52% 的电流密度衰减. Dodelet 等[54]发现 Fe-N-C 催化剂在燃料电池测试初期 100 小时内发生将近 50% 的衰减, 此阶段的快速衰减是由于微孔水淹造成的 Fe-N₄ 活性位点的脱离[55]. 目前, 非贵金属催化剂的性能衰减机制仍然不明确. 可能原因除了质子化效应[56]和金属活性中心在酸性电解质中溶解外[57], 还有: 1)与 Pt 基催化剂相比, 非贵金属催化剂尤其是 Fe-N-C 催化剂的氧还原会生成更多的过氧化氢中间产物, 过氧化氢在局部位置的累积不仅会加速氧化、腐蚀催化剂活性中心和碳基体, 而且还会使质子交换膜发生降解[58]; 2)

较厚的非贵金属催化剂层不利于水管理, 氧还原反应生成的水不能有效排出、堵塞催化剂微孔, 影响氧气传质[59-60].

Fe-N-C 催化剂容易发生 Fenton 反应产生羟基和过氧化氢自由基导致催化层的退化, 而 Co-N-C[11, 47, 55]和 Mn-N-C[49]等表现出更好的耐久性. 如图 5A 所示, Co-N-C 在 0.4 V、0.5 V 和 0.7 V 的电位下表现出比 Fe-N-C 的更好的电流稳定性, 尤其是在 0.4 V 的低电位下进行 20 h 测试, Co-N-C 仍保持了 60% 的初始电流密度而 Fe-N-C 只能保持 25%[47]. 但是 Co-N-C 上过氧化氢产率较大, 易造成膜电极的破坏, 因此需要进一步提高 Co-N-C 催化剂的活性和选择性. Mn-N-C 的耐久性比 Co-N-C 和 Fe-N-C 优异(图 5B), Mn 的掺杂有利于提高碳载体的稳定性, 但其活性仍需要大幅度的改善. 不同的 Fe-N、Co-N 和 Mn-N 键的金属活性位点稳定性溶解机制可能不同, 双金属掺杂如 Fe-Mn-N-C[61]和 Fe-Co-N-C[53, 62]催化剂的发展也在一定程度上提高了非贵金属催化剂的稳定性.

5 结论与展望

非贵金属催化剂的发展和应用可以大大降低催化剂成本, 有助于推动燃料电池商业化进程. 本综述从催化剂设计构筑、催化层结构优化、电池测试条件以及耐久性四个方面详细介绍了近年来 M-N-C 型非贵金属 ORR 催化剂研究所取得的代表性进展. 虽然 M-N-C 型非贵金属催化剂在性能上取得了很大突破, 基于 Fe-N-C 催化剂的燃料电池最大功率密度高达 1.18 W·cm⁻², 可以与低载量(0.1 mg·cm⁻²)Pt/C 催化剂燃料电池的最大功率密度相媲美, 但其单位体积比活性和耐久性目前与 Pt 基催化剂相比还存在较大差距. 优化 M-N-C 催化剂的合成步骤实现规模化生产的同时保证单原子活性位点的均匀分散减少金属碳化物及金属颗粒的形成是实现非贵金属催化剂走向实用的另一挑战.

为了改善催化层过厚所引发的性能提升瓶颈和耐久性问题, 今后需要在以下几个方面进行深入系统研究: 1)非贵金属催化剂的设计构筑不仅需要提升其单位体积的活性位点密度, 还应着眼于调控催化剂的孔隙结构和表面的亲疏水特性, 以提升活性位点的有效利用率; 2)优化催化剂浆料组成和催化剂分散状态以及膜电极制备工艺的同时, 应结合先进的表征技术深入研究催化层内
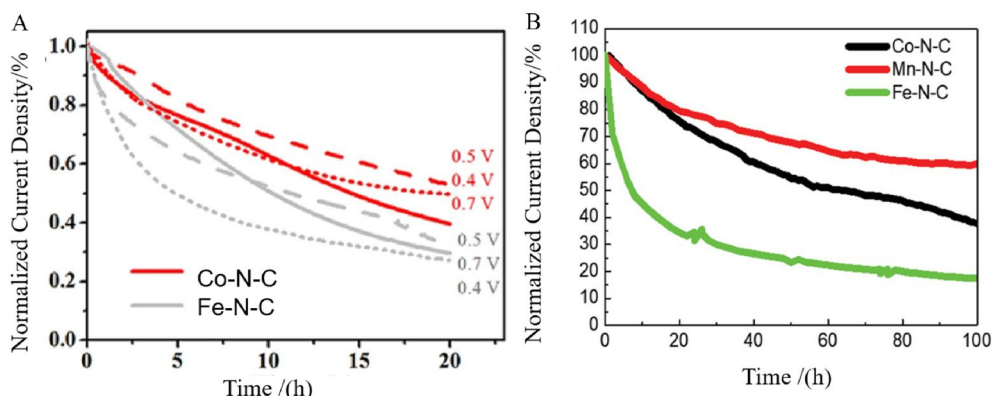
图 5　(A) 燃料电池测试中 Co-N-C 和 Fe-N-C 在 0.4 V(点线), 0.5 V (虚线)和 0.7 V (实线)电位下的电流密度稳定性[47]. (B) 燃料电池测试中在 0.7 V 电位下 Co-N-C(黑线), Mn-N-C(红线)和 Fe-N-C (绿线)的电流密度稳定性[60].

Fig. 5　(A) Current stability curves of Co-N-C(red) and Fe-N-C(grey) catalysts at voltages of 0.4 V (dot), 0.5 V (dash) and 0.7 V (solid)[47]. (B) Current stability curves of Co-N-C (black), Mn-N-C (red) and Fe-N-C (green) catalysts at voltage of 0.7 V[60].

催化剂和离聚物在三维尺度上的分布状态，最大化三相反应界面、完善水管理，提升反应过程中的氧气传输和质子传输效率，减小电极欧姆极化和浓差极化，只有这样非贵金属催化剂的性能才能在整个电流密度区间与 Pt 基催化剂匹敌；3）目前，非贵金属催化剂面临的最大挑战是耐久性问题，关于其衰减机制的研究需要更加全面地进行，结合实际燃料电池运行条件，综合评估催化剂活性位点、碳骨架以及催化层的稳定性，从而寻找到有效的应对策略.

参考文献(References)：

[1] Cano Z P, Banham D, Ye S Y, et al. Batteries and fuel cells for emerging electric vehicle markets[J]. Nature Energy, 2018, 3(4): 279-289.

[2] Adzic R R, Zhang J, Sasaki K, et al. Platinum monolayer fuel cell electrocatalysts[J]. Topics in Catalysis, 2007, 46 (3/4): 249-262.

[3] Shao M H, Shoemaker K, Peles A, et al. Pt monolayer on porous Pd-Cu alloys as oxygen reduction electrocatalysts [J]. Journal of the American Chemical Society, 2010, 132 (27): 9253-9255.

[4] Shao M H, Chang Q W, Dodelet J P, et al. Recent advances in electrocatalysts for oxygen reduction reaction[J]. Chemical Reviews, 2016, 116(6): 3594-3657.

[5] Ioroi T, Siroma Z, Yamazaki S I, et al. Electrocatalysts for PEM fuel cells[J]. Advanced Energy Materials, 2018, 9(23): 1801284.

[6] Zhao Z P, Chen C L, Liu Z Y, et al. Pt-based nanocrystal for electrocatalytic oxygen reduction[J]. Advanced Materi-als, 2019, 31(31): 1808115.

[7] Akita T, Taniguchi A, Maekawa J, et al. Analytical TEM study of Pt particle deposition in the proton-exchange membrane of a membrane-electrode-assembly[J]. Journal of Power Sources, 2006, 159(1): 461-467.

[8] Xiao F, Xu G L, Sun C J, et al. Nitrogen-coordinated single iron atom catalysts derived from metal organic frameworks for oxygen reduction reaction[J]. Nano Energy, 2019, 61: 60-68.

[9] Li J C, Xiao F, Zhong H, et al. Secondary-atom-assisted synthesis of single iron atoms anchored on N-doped carbon nanowires for oxygen reduction reaction[J]. ACS Catalysis, 2019, 9(7): 5929-5934.

[10] Wan X, Liu X F, Li Y C, et al. Fe-N-C electrocatalyst with dense active sites and efficient mass transport for high-performance proton exchange membrane fuel cells [J]. Nature Catalysis, 2019, 2(3): 259-268.

[11] Wang X X, Cullen D A, Pan Y T, et al. Nitrogen-coordi-nated single cobalt atom catalysts for oxygen reduction in proton exchange membrane fuel cells[J]. Advanced Mat-erials, 2018, 30(11): 1706758.

[12] Wang X X, Swihart M T, Wu G. Achievements, chal-lenges and perspectives on cathode catalysts in proton ex-change membrane fuel cells for transportation[J]. Nature Catalysis, 2019, 2(7): 578-589.

[13] Martinez U, Komini Babu S, Holby E F, et al. Progress in the development of Fe-based PGM-free electrocatalysts for the oxygen reduction reaction[J]. Advanced Materials, 2019, 31(31): 1806545.

[14] Zhang H B, Liu G G, Shi L, et al. Single-atom catalysts: emerging multifunctional materials in heterogeneous

catalysis [J]. Advanced Energy Materials, 2018, 8 (1): 1701343.

[15]　Zhang H G, Osgood H, Xie X H, et al. Engineering nanostructures of PGM-free oxygen-reduction catalysts using metal-organic frameworks[J]. Nano Energy, 2017, 31: 331-350.

[16]　Banham D, Ye S Y, Pei K, et al. A review of the stability and durability of non-precious metal catalysts for the oxygen reduction reaction in proton exchange membrane fuel cells[J]. Journal of Power Sources, 2015, 285: 334-348.

[17]　ZhangY L(张雅琳), Chen C(陈驰), Zhou L L(邹亮亮), et al. Fe-N doped hollow carbon nanospheres linked by carbon nanotubes for oxygen reduction reaction[J]. Journal of Electrochemistry(电化学), 2018, 24(6): 726-732.

[18]　Liu J(刘京), Ran G J(冉光钧), Ruan M B(阮明波), et al. Recent research progress for non-Pt-based oxygen reduction reaction electrocatalysts in fuel cell[J]. Journal of Electrochemistry(电化学), 2015, 21(2): 130-137.

[19]　Yang X H, Wang Y C, Zhang G X, et al. SiO$_2$-Fe/N/C catalyst with enhanced mass transport in PEM fuel cells [J]. Applied Catalysis B: Environ mental, 2020, 264: 118523.

[20]　Zhan Y F, Zeng H B, Xie F Y, et al. Templated growth of Fe/N/C catalyst on hierarchically porous carbon for oxygen reduction reaction in proton exchange membrane fuel cells[J]. Journal of Power Sources, 2019, 431: 31-39.

[21]　Qiu J S(邱介山), Wang Z Y(王治宇), Xiu L Y(修陆洋), et al. Caging porous Co-N-C nanocomposites in 3D graphene as active and aggregation-resistant electrocatalyst for oxygen reduction reaction[J]. Journal of Electrochemistry(电化学), 2018, 24(6): 715-725.

[22]　Barkholtz H M, Chong L, Kaiser Z B, et al. Highly active non-PGM catalysts prepared from metal organic frameworks[J]. Catalysts, 2015, 5(2): 955-965.

[23]　Zhao D, Shui J L, Grabstanowicz L R, et al. Highly efficient non-precious metal electrocatalysts prepared from one-pot synthesized zeolitic imidazolate frameworks [J]. Advanced Materials, 2014, 26(7): 1093-1097.

[24]　Barkholtz H M, Chong L, Kaiser Z B, et al. Enhanced performance of non-PGM catalysts in air operated PEM-fuel cells[J]. International Journal of Hydrogen Energy, 2016, 41(47): 22598-22604.

[25]　Zhao D, Shui J L, Grabstanowicz L R, et al. A versatile preparation of highly active ZIF-based non-PGM catalysts through solid state synthesis[J]. ECS Transactions, 2014, 64(3): 253-260.

[26]　Barkholtz H, Chong L, Kaiser Z B, et al. Non-precious metal catalysts prepared by zeolitic imidazolate frameworks: The ligand influence to morphology and performance[J]. Fuel Cells, 2016, 16(4): 428-433.

[27]　Yuan S, Shui J L, Grabstanowicz L, et al. A highly active and support-free oxygen reduction catalyst prepared from ultrahigh-surface-area porous polyporphyrin[J]. Angewandte Chemie International Edition, 2013, 52(32): 8349-8353.

[28]　Shui J L, Chen C, Grabstanowicz L, et al. Highly efficient nonprecious metal catalyst prepared with metal-organic framework in a continuous carbon nanofibrous network [J]. Proceedings of the National Academy of Sciences, 2015, 112(34): 10629-10634.

[29]　Li Y C, Liu X F, Zheng L R, et al. Preparation of Fe-N-C catalysts with FeN$_x$ (x = 1, 3, 4) active sites and comparison of their activities for the oxygen reduction reaction and performances in proton exchange membrane fuel cells[J]. Journal of Materials Chemistry A, 2019, 7(45): 26147-26153.

[30]　Chen J R, Yan X H, Fu C H, et al. Insight into the rapid degradation behavior of nonprecious metal Fe-N-C electrocatalyst-based proton exchange membrane fuel cells [J]. ACS Applied Materials & Interfaces, 2019, 11 (41): 37779-37786.

[31]　Li J, Bruller S, Sabarirajan D C, et al. Designing the 3D architecture of PGM-free cathodes for H$_2$/air proton exchange membrane fuel cells[J]. ACS Applied Energy Materials, 2019, 2(10): 7211-7222.

[32]　Li W, Ding W, Nie Y, et al. Transformation of metal-organic frameworks into huge-diameter carbon nanotubes with high performance in proton exchange membrane fuel cells[J]. ACS Applied Materials & Interfaces, 2019;11 (25): 22290-22296.

[33]　Workman M J, Serov A, Tsui L K, et al. Fe-N-C catalyst graphitic layer structure and fuel cell performance [J]. ACS Energy Letters, 2017, 2(7): 1489-1493.

[34]　Wang J, Huang Z Q, Liu W, et al. Design of N-coordinated dual-metal sites: a stable and active Pt-free catalyst for acidic oxygen reduction reaction[J]. Journal of the American Chemical Society, 2017, 139(48): 17281-17284.

[35]　Chung H T, Cullen D A, Higgins D, et al. Direct atomic-level insight into the active sites of a high-performance PGM-free ORR catalyst[J]. Science, 2017, 357(6350):479-484.

[36]　Wang W, Chen W H, Miao P Y, et al. NaCl crystallites as dual-functional and water-removable templates to synthesize a three-dimensional graphene-like macroporous Fe-NC catalyst[J]. ACS Catalysis, 2017, 7(9): 6144-6149.

[37] Sa Y J, Seo D J, Woo J, et al. A general approach to preferential formation of active Fe-N$_x$ sites in Fe-N/C electrocatalysts for efficient oxygen reduction reaction[J]. Journal of the American Chemical Society, 2016, 138 (45): 15046-15056.

[38] Zhang N, Zhou T P, Chen M L, et al. High-purity pyrrole-type FeN$_4$ sites as a superior oxygen reduction electrocatalyst[J]. Energy & Environmental Science, 2020, 13 (1): 111-118.

[39] Li J Z, Zhang H G, Samarakoon W, et al. Thermally driven structure and performance evolution of atomically dispersed FeN$_4$ sites for oxygen reduction[J]. Angewandte Chemie International Edition, 2019, 58(52): 18971-18980.

[40] Qiao M F, Wang Y, Wang Q, et al. Hierarchically ordered porous carbon with atomically dispersed FeN$_4$ for ultra-efficient oxygen reduction reaction in PEMFC[J]. Angewandte Chemie International Edition, 2019, 59(7): 2688-2694.

[41] Fu X G, Li N, Ren B H, et al. Tailoring FeN$_4$ sites with edge enrichment for boosted oxygen reduction performance in proton exchange membrane fuel cell[J]. Advanced Energy Materials, 2019, 9(11): 1803737.

[42] Wang Q, Zhou Z Y, Lai Y J, et al. Phenylenediamine-based FeN$_x$/C catalyst with high activity for oxygen reduction in acid medium and its active-site probing [J]. Journal of the American chemical Society, 2014, 136 (31): 10882-10885.

[43] Zhang H, Chung H T, Cullen D A, et al. High-performance fuel cell cathodes exclusively containing atomically dispersed iron active sites[J]. Energy & Environmental Science, 2019, 12(8): 2548-2558.

[44] Zhang G X, Yang X H, Dubois M, et al. Non-PGM electrocatalysts for PEM fuel cells: effect of fluorination on the activity and stability of a highly active NC_Ar$^+$+NH$_3$ catalyst[J]. Energy & Environmental Science, 2019, 12 (10): 3015-3037.

[45] Tian J, Morozan A, Sougrati M T, et al. Optimized synthesis of Fe/N/C cathode catalysts for PEM fuel cells: a matter of iron-ligand coordination strength[J]. Angewandte Chemie International Edition, 2013, 52(27): 6867-6870.

[46] Chong L, Goenaga G A, Williams K, et al. Investigation of oxygen reduction activity of catalysts derived from Co and Co/Zn methyl-imidazolate frameworks in proton exchange membrane fuel cells[J]. ChemElectroChem, 2016, 3(10): 1541-1545.

[47] Chen L Y, Liu X F, Zheng L R, et al. Insights into the role of active site density in the fuel cell performance of Co-NC catalysts[J]. Applied Catalysis B: Environmental, 2019, 256: UNSP117849.

[48] He Y, Hwang S, Cullen D A, et al. Highly active atomically dispersed CoN$_4$ fuel cell cathode catalysts derived from surfactant-assisted MOFs: carbon-shell confinement strategy[J]. Energy & Environmental Science, 2019, 12(1): 250-260.

[49] Li J, Chen M, Cullen D A, et al. Atomically dispersed manganese catalysts for oxygen reduction in proton-exchange membrane fuel cells[J]. Nature Catalysis, 2018, 1 (12): 935-945.

[50] Banham D, Kishimoto T, Zhou Y G, et al. Critical advancements in achieving high power and stable non-precious metal catalyst-based MEAs for real-world proton exchange membrane fuel cell applications[J]. Science Advances, 2018, 4(3): eaar7180.

[51] Shao Y, Dodelet J P, Wu G, et al. PGM-free cathode catalysts for PEM fuel cells: A mini-review on stability challenges[J]. Advanced Materials, 2019, 31(31): 1807615.

[52] Serov A, Workman M J, Artyushkova K, et al. Highly stable precious metal-free cathode catalyst for fuel cell application[J]. Journal of Power Sources, 2016, 327: 557-564.

[53] Wu G, More K L, Johnston C M, et al. High-performance electrocatalysts for oxygen reduction derived from polyaniline, iron, and cobalt[J]. Science, 2011, 332(6028): 443-447.

[54] Proietti E, Jaouen F, Lefèvre M, et al. Iron-based cathode catalyst with enhanced power density in polymer electrolyte membrane fuel cells[J]. Nature Communication, 2011, 2: 416.

[55] Chenitz R, Kramm U I, Lefèvre M, et al. A specific demetalation of Fe-N$_4$ catalytic sites in the micropores of NC_Ar + NH$_3$ is at the origin of the initial activity loss of the highly active Fe/N/C catalyst used for the reduction of oxygen in PEM fuel cells[J]. Energy & Environmental Science, 2018, 11(2): 365-382.

[56] Martinez U, Babu S K, Holby E F, et al. Durability challenges and perspective in the development of PGM-free electrocatalysts for the oxygen reduction reaction[J]. Current Opinion in Electrochemistry, 2018, 9: 224-232.

[57] Choi C H, Baldizzone C, Grote J P, et al. Stability of Fe-N-C catalysts in acidic medium studied by operando spectroscopy[J]. Angewandte Chemie International Edition, 2015, 54(43): 12753-12757.

[58] Choi C H, Lim H K, Chung M W, et al. The Achilles' heel of iron-based catalysts during oxygen reduction in an acidic medium[J]. Energy & Environmental Science, 2018, 11(11): 3176-3182.

[59] Zhang G X, Chenitz R, Lefèvre M, et al. Is iron involved

in the lack of stability of Fe/N/C electrocatalysts used to reduce oxygen at the cathode of PEM fuel cells?[J].Nano Energy, 2016, 29: 111-125.

[60] Du L, Prabhakaran V, Xie X H, et al. Low-PGM and PGM-free catalysts for proton exchange membrane fuel cells: Stability challenges and material solutions[J]. Advanced Materials, 2020: 1908232. DOI: 10.1002/adma.201908232.

[61] Sahraie N R, Kramm U I, Steinberg J, et al. Quantifying the density and utilization of active sites in non-precious metal oxygen electroreduction catalysts[J]. Nature Communication, 2015, 6(1): 1-9.

[62] Wang J, Huang Z Q, Liu W, et al. Design of N-coordinated dual-metal sites: A stable and active Pt-free catalyst for acidic oxygen reduction reaction[J]. Journal of the American Chemical Society, 2017, 139(48): 17281-17284.

Fuel Cell Performance of Non-Precious Metal Based Electrocatalysts

ZHANG Yan-feng[1,2,3,4a], XIAO Fei[2a], CHEN Guang-yu[2,5a], SHAO Min-hua[2,5,6*]

(1. *Jiangsu Aoxin NEV Co., Ltd, Yancheng, Jiangsu, 224000, China*; 2. *Department of Chemical and Biological Engineering, Hong Kong University of Science and Technology, Clear Water Bay, Kowloon, Hong Kong, China*; 3. *Shanghai AI NEV Innovative Platform Co., Ltd, Shanghai*, 201805, *China*; 4. *Yangtse Delta Academy of NEV CO.,LTD, Yancheng, Jiangsu*, 224000, *China*; 5. *Fok Ying Tung Research Institute, The Hong Kong University of Science and Technology, Guangzhou* 511458, *China*; 6. *Energy Institute, The Hong Kong University of Science and Technology, Clear Water Bay, Kowloon, Hong Kong* 999077, *China*)

Abstract: The commercialization of proton exchange membrane fuel cells (PEMFCs) is hindered by high cost and low durability of Pt based electrocatalysts. Developing efficient and durable non-precious metal catalysts is a promising approach to addressing these conundrums. Among them, transition metals dispersed in a nitrogen (N)-doped carbon support (M-N-C) show good oxygen reduction reaction activity. This article reviews recent progress in M-N-C catalysts development, focusing on the catalysts design, membrane electrode assembly fabrication, fuel cell performance, and durability testing. Template-assisted approach is an efficient way to synthesize M-N-C materials with homogeneously dispersed single atom active site and reduced metal particles, carbides formation. However, the issue related to low intensity of active sites should be addressed via strengthening metal-ligand interaction and using high surface area precursors. In general, the catalyst loading for the membrane electrode assembly (MEA) of non-precious catalyst is high $(3 \sim 4 \ mg \cdot cm^{-2})$ in order to obtain acceptable performance, which is also highly dependent on ink preparation and coating protocol, ionomer/catalyst ratio, etc. The highest power densities for Fe-N-C and Co-N-C are reported to be 1.18 and 0.87 $W \cdot cm^{-2}$ with O_2 at the cathode, respectively. Despite the significant progress in non-precious metal catalysts development, the undesired durability (only a few hundreds of hours) is still far from the target of 5000 h by 2025. Thus, much more efforts should be spent on improving their durability.

Key words: proton exchange membrane fuel cells; non-precious metal catalysts; membrane electrode assembly; durability